이학석사 학위 논문

염기 교정과 프라임 교정 기술을 이용하여 레쉬-니한 증후군의 치료학적인 유전자 편집

Therapeutic genome editing for Lesch-Nyhan Syndrome using Base and Prime editors

울 산 대 학 교 대 학 원

의 과 학 과

장 가 영

Therapeutic genome editing for Lesch-Nyhan Syndrome using Base and Prime editors

지 도 교 수 김 용 섭

이 논문을 이학석사학위 논문으로 제출함

2022년 2월

울 산 대 학 교 대 학 원

의 과 학 과

장 가 영

장가영의 이학석사학위 논문을 인준함

심사위원 장 수 환(인)

심사위원 최 은 영(인)

심사위원 김 용 섭(인)

울 산 대 학 교 대 학 원

2022년 2월

Acknowledgements

I would like to thank Prof. Beom Hee Lee, Hyosang Do and Sun Hee Heo for helping in LNS research. I also thank our Genome Engineering & Molecular Genetics laboratory members including Dr. Jiyeon Kwon for their experimental help and comments.

Abstract

Inherited human genetic disorders are mostly caused by nucleotide alteration in an associated gene or its regulatory elements. There are various types of nucleotide alterations in the genome such as point mutations, insertions, and deletions. Introduction and correction these nucleotide alterations in living cells and organisms are great challenging to manage the human genetic diseases. Although the conventional CRISPR-based nuclease has been developed and widely applied to treat genes associated with various genetic diseases, the nuclease-based gene editing to correct targeted mutation has several limitations such as low correction frequency, generation of DNA double-strand breaks, and requirement of donor DNA template. To overcome these limitations, recent studies show that CRISPR-mediated base and prime editors allows editing of desired mutations in the genome.

Lesch-Nyhan Syndrome (LNS) well known as rare genetic disease is caused by hypoxanthine-guanine phosphoribosyl transferase 1 (*HPRT1*) gene mutation. A *HPRT1* deficiency causes hyperuricemia and a various spectrum of neurological symptoms such as motor dysfunctions, cognitive impairment, and behavioral disorder. Although the causal role of *HPRT1* has been confirmed over the past 50 years, there is no fundamental treatment for LNS patients. To provide proof-of-concept evidence regarding the feasibility of CRISPR based gene therapy, I applied CRISPR-mediated base and prime editors to correct LNS-related *HPRT1* gene mutation. I generated several cell lines which introduced LNS patient-derived mutations including c.333_334ins(A), c.430C>T, and c.508C>T with optimized base and prime editors.

Then I also corrected these mutations in the cells up to 46.7% and generated corrected cell lines. Furthermore, I analyzed the function of HPRT1 in these established cell lines and confirmed that HPRT1 functions are fully disrupted in the mutant cells and rescued in corrected cells. From these results, I first suggest that CRISPR-mediated base and prime editors can be used for generating LNS model cells and treating the disease by *HPRT1* gene correction. These genome editing tools could be widely used to treatment of various types of genetic mutation in LNS patients.

Key word: Lesch-Nyhan Syndrome, HPRT1, CRISPR-Cas9, Base Editing, Prime Editing, Genome editing, Gene therapy

Contents

List of tables and figures

Introduction

Lesch-Nyhan Syndrome (LNS) is an uncommon X-linked recessive disease in which the purine salvage enzyme hypoxanthine-guanine phosphoribosyl transferase1 (HPRT1) is completely inactivated [1]. Using 5'-phosphoribosyl-1-pyrophosphate (PRPP) as a co-substrate, *HPRT1* mediates the salvage pathway of inosine monophosphate (IMP) and guanosine monophosphate (GMP) from hypoxanthine and guanine purine bases. *HPRT1* deficiency induces the accumulation of hypoxanthine and guanine, which are substrates of enzymes, and these substrates are oxidized into uric acid by xanthine oxidase. Purine synthesis is promoted by increased availability of PRPP for PRPP amidotransferase in de novo synthesis of purine nucleotides. On the other hand, the synthesis of PRPP amidotransferase feedback inhibitors such as IMP and GMP is reduced. The increased de novo synthesis of purine nucleotides occurs from this process. Overproduction of uric acid in *HPRT1* deficiency is characterized by a combination of purine base recycling and excessive purine nucleotide synthesis. As a result, patients with LNS show excessive purine production and associated neurological manifestations, such as compulsive self-mutilation, choreoathetosis, spasticity, and developmental delay [2-5].

Among the treatments for Lesch-Nyhan syndrome, allopurinol can prevent hyperuricemia by inhibiting uric acid production, but it did not affect neurodevelopment or cognitive outcomes [6]. Because there is no adequate hypothesis to explain the neurological symptoms of LNS, it is difficult to create a rational treatment, and effective LNS treatment is absent, even though the role of *HPRT1* has been confirmed

for nearly 50 years [6-7]. So, I applied CRISPR-mediated genome editing technology to correct LNS-related *HPRT1* gene mutations.

Conventional CRISPR-Cas9 system can be utilized to correct undesirable genes that linked genetic disorders and has developed and applied to many biological studies and field of gene therapy. The Cas9 and gRNA complex generate double strand breaks (DSBs) at the target region. Damaged DNA is repaired by non-homologous end joining (NHEJ) and homology directed repair (HDR) systems. NHEJ pathway connects the DNA cut site as it is, and the insertion or deletions of the base sequence is induced. Homology directed repair (HDR), which uses DNA with the same sequence as a template to repair the cut area accurately without errors such as insertions or deletions of the sequence. However, NHEJ pathway occurs much more frequently in most cell types, and HDR is less efficient, so there are limitations in targeting various diseases [8-12]. Also, it is difficult to edit point mutations, which hinders its therapeutic application. So, to overcome this limitation, CRISPR-mediated base editors (BEs) and prime editors (PEs) were developed. The BE is in the form of nCas9 and deaminase fusion, which is targeted point mutation by nicking the target DNA without the donor DNA template and DSBs. There are two types of BEs: cytosine base editor (CBE) and adenine base editor (ABE). CBE and ABE catalyze C to T and A to G conversion, respectively, and enable editing of transition mutations [13-16]. However, BEs are unable to induce transversion mutation editing as well as insertion and deletion, and undesired bystander alternation is induced within the base editing window at the target site [17]. The prime editor 2 (PE2) is a revolutionary genome-editing technique that can make accurate point mutations in the genome without requiring a DSB or

donor DNA templates. A PE2 is a fusion protein composed of an engineered reverse transcriptase (RT) and a catalytically depleted SpCas9 nickase (H840A). A primer binding site (PBS) and reverse transcriptase template are encoded by a prime editing guide RNA (pegRNA), which directs the PE to the appropriate genomic region and allows the RT to transcribe the additional genetic code into the target genomic locus. Prime editing introduces all 12 patterns of point mutations as well as small insertions and small deletions in an accurate. The PE3 and PE3b systems increase editing efficiency by introducing additional gRNA to nick the non-edited DNA strand to facilitate the edited strand to be used as a repair template [18-23]. Therefore, base editing and prime editing can be used to target disease-associated genes for gene therapy.

In this study, I establish a LNS disease model with patient-derived mutations and use BE and PE to correct mutagenic LNS to demonstrate functional correction of *HPRT1* mutations. As a result, these data demonstrate the potential for treatment of Lesch-Nyhan Syndrome by verifying efficiently corrected mutant cells.

Materials and method

Analysis of targetable disease mutations in *HPRT1*

The *HPRT1* variations database (www.Lesch-Nyhan.org) was used to obtain LNS-related variants. The National Center for Biotechnology Information (NCBI) website provided information on the reference sequence and CDS region of each mutation. The graph shows the coverage frequency of BEs and PEs capable of editing mutations in *HPRT1* gene, and the target range of PEs is insertion of less than 40bp and deletion of less than 80bp.

Plasmids and Cloning

The gRNAs were cloned into the Bsa1-HFv2 (New England BioLabs, USA) digested pRG2 (Addgene plasmid #104174) vector. The pegRNAs were cloned into the Bsa1-HFv2 (New England BioLabs) digested pU6-pegRNAGG-acceptor (Addgene plasmid #132777), and the pegRNA sequences are listed in Table 2. Using acceptor plasmids, Gibson or Golden Gate assembly was used to create plasmids expressing pegRNAs. In the plasmid DNA transfection studies, pCMV-BE3 (Addgene plasmid #73021), pCMV-BE4max_3xHA (Addgene plasmid #112096), pCMV-AncBE4max (Addgene plasmid #112094), xCas9(3.7)-BE4 (Addgene plasmid #108381), pCAG-CBE4max-SpCas9-NG-P2A-EGFP (Addgene plasmid #140001), pCMV-T7-ABEmax(7.10)-SpG-P2A-EGFP (Addgene plasmid #140002), pCAG-CBE4max-SpRY-P2A-EGFP (Addgene plasmid #139999), pCAG-CBE4max-SpG-P2A-EGFP (Addgene plasmid #139998), pCMV-T7-ABEmax(7.10)-SpCas9-NG-P2A-EGFP (Addgene plasmid #140005), pCMV-T7-ABEmax(7.10)-SpRY-P2A-EGFP (Addgene plasmid #140003), pCMV-

T7-ABEmax(7.10)-xCas9(3.7)-P2A-EGFP (Addgene plasmid #140004) and pCMV-PE2 (Addgene plasmid #132775) were used.

Cell culture and Transfection

HEK293T/17 (ATCC CRL-11268) cells were cultured in Dulbecco's modified Eagle's medium and HAP1 cells were cultured in Iscove's modified Dulbecco's medium supplemented with 10% fetal bovine serum and 1% penicillin/streptomycin (Thermo Fisher Scientific, USA). 1 day before transfection, HEK293T/17 cells were seeded at 1.5×10^5 cells and HAP1 cells were seeded at 0.8×10^5 cells per well density onto a TC-treated 24-well plate (Corning Life Sciences, USA). At approximately 60-70% cell confluency, 2㎍ of plasmids and 3㎕ of Lipofectamine 2000 (Thermo Fisher Scientific, USA) were transfected according to the manufacturer's protocol. PEs or BEs (1.5㎍) and pegRNAs or sgRNA-encoding plasmid (500ng) were used. In the PE3 and PE3b studies, the PE2 (1.5㎍) and pegRNA (500ng) plasmids were transfected with sgRNA (166ng).

Construction of *HPRT1* mutant-HEK293T/17 cell lines

1ug of plasmid DNA (500ng lenti HPRT1 mutant viral vector, 300ng psPAX2, and 200ng pMD2.G) were transfected in 2×10^5 HEK293T/17 cells which are seeded in 24-well plates following the manufacturer's directions with Lipofectamine 2000 (Invitrogen, USA). The culture medium was replaced 24 hours after transfection, and lentiviruses were obtained 48 hours later and filtered with a 0.45μM filter (Merck Milipore, USA). The HEK293T/17 cells were transduced with various quantities of lentivirus supernatant, and the infected cells were selected 24 hours later with a

2㎍/ml puromycin treatment. Each lentivirus condition's cell viability was assessed 72 hours after puromycin selection and compared to cells that had not been puromycin selected. Cells of lentivirus conditions with a low multiplicity of infection were selected.

Construction of *HPRT1* mutant and rescued-HAP1 cell lines

The transfected cells with BEs and gRNA plasmid or PEs and pegRNA plasmid were treated with 6-Thioguanine(6-TG) (Sigma-Aldrich, USA) and 50× Hybri-Max HAT Media Supplement (Sigma-Aldrich, USA) drug. The cells were selected for 10 days with 10㎍/ml 6-TG and HAT Media Supplement-containing media.

Sanger sequencing

Genomic DNA is extracted using DNA Blood & Tissue kit (Qiagen, USA) according to the manufacturer's protocol from defective cell lines and repaired cell lines for each of the three *HPRT1* mutations. PCR primers were used to amplify the *HPRT1* gene. The primer sequences are listed in Table 5.

Targeted deep sequencing and data analysis

Three rounds of PCR were used to amplify the target sites and the size of the PCR amplicon was validated on a 2 percent agarose gel. The amplicons were sequenced using the Illumina MiniSeq or iSeq 100 sequencing systems at 150-bp paired-end. The fastq-join tool (https://github.com/brwnj/fastq-join) was used to join the paired-end reads. MAUND (https://github.com/ibscge/maund) was used for targeted deep sequencing analysis and confirmed by Cas-Analyzer (http://www.rgenome.net/cas-

analyzer). BE-Analyzer (http://www.rgenome.net/be-analyzer/), a tool for analyzing base editing efficiency, was also used to confirm the results. PCR primers were used to amplify the *HPRT1* gene. The primer sequences are listed in Table 5.

Drug selection

The 6-TG and HAT Media Supplement was added to the supplemented IMDM for HPRT1 mutant and rescued cell selection. The cells were cultured for 3 days with 10μg/ml 6-TG and HAT Media Supplement-containing media.

Crystal violet staining

The *HPRT1* defective and repaired cells were seeded in 24-well plates at 1.5×10^5 and cultured in medium supplemented 10μg/ml 6-TG or HAT. The media supernatant was removed after 3 days and treated with 4 percent paraformaldehyde (Biosesang, Korea). The cells were then stained for 20 minutes with a 1% crystal violet staining solution (Sigma Aldrich, USA).

Results

1. *HPRT1* mutation analysis in worldwide databases.

First, I investigated *HPRT1* mutation associated with the known Lesch-Nyhan syndrome. According to the Lesch-Nyhan disease international study group [24], a total of 615 *HPRT1* gene variants causing LNS have been registered, the majority of the *HPRT1* gene mutation types identified are point mutation, deletion, and duplication. Among the *HPRT1* mutation types, 29.9% are deletion and duplication mutations and 61.9% are transition point mutations and transversion point mutation (Fig. 1A). BEs and PEs coverage frequency that can be edited by targeting *HPRT1* mutation were also examined. CBE and ABE can target 17.7% (C>T or G>A) and 12.8% (A>G or T>C) of the *HPRT1* point mutations, respectively. PEs can edit insertions of 44bp or less and deletions of 80bp or less at the target site [18]. Considering this, prime editing can cover 92.1% of transversion point mutations, deletion, and duplication as well as transition point mutations that CBE and ABE can target (Fig. 1B). These data analysis indicated that most of the LNS-causing *HPRT1* mutations can be targeted using BEs and PEs.

2. Development of mutant and rescued cell lines using base editing.

I selected two types of patient-derived mutations: c.430C>T and c.508C>T and these mutations lead to the premature stop codon. I used CBE to make the LNS disease model and ABE to repair the disease-causing mutation (Fig. 2). To generate an LNS disease model, the gRNAs were designed by targeting C in the editing window to overcome bystander alteration. Using each plasmid encoding gRNAs, cytosine can be converted to thymidine at the template strand at the 5^{th} and 6^{th} at the target sites, respectively (Fig 3). To correct an *HPRT1* disease causing mutation, I also designed correction gRNA which recognize NG-PAM. Conversion of A to G in the template strand, resulting in T-to-C correction on the coding strand, would repair the pathogenic mutation at position 5 (starting from the 5' end of the target sequence) in the target site (Fig. 3). To select the most efficient BE variant for further experiments, BE optimization was performed. The mutation induced encoding gRNA plasmid and several BEs systems were co-transfected in HEK293T/17 cell for 72 hours. The editing activity of AncBE4max and BE4max-SpG system was 9.1% and 6.7% with the highest editing efficiency, respectively (Fig. 4). Likewise, to test BEs optimization for correction of disease mutation, gRNA plasmid and several BEs systems were co-transfected in *HPRT1* mutant-HEK293T cell. The highest base editing frequency of ABEmax-xCas9(3.7) and ABEmax-SpG system was the 2.1% and 5.3%, respectively (Fig. 5). Next, to establish deficiency cell lines, HAP1 cells were transfected with the AncBE4max plasmid or BE4max-SpG plasmid and sgRNA plasmid and harvested on 3 days. The transfected cells were treated with 6-TG which is selected for HPRT1 gene-disrupted cells [25-28]. ABEmax-xCas9(3.7) or ABEmax-SpG plasmid and

gRNA plasmid were transfected into *HPRT1* deficient-HAP1 cells after selection was completed, and the rescued cell line was established by selection with the HAT drug used for wild-type cell selection [29]. Genomic DNA was extracted from the obtained cell and amino acid conversion was identified by sanger sequencing (Fig. 6) I also used targeted deep sequencing to evaluate potential off-target sites predicted in mutant and rescued cell lines. As potential off-target sites, spacer sequences with mismatches≤2 and NGG or NG PAM were considered. Off-target effects were almost undetectable at 9 potential off-target sites (Fig. 7). To examined whether HPRT1 function is present in the established cell, drug selection and protein expression were observed. After selecting 6-TG and HAT drugs, the broken and restored function could be proven (Fig. 8), as well as abnormal and normal HPRT1 protein expression (Fig. 9). These results demonstrated that it was possible to efficiently make mutant and rescued cell lines with impaired and repaired HPRT1 function using base editing, respectively.

3. Installation and correction of *HPRT1* mutation using prime editing.

Another patient-derived mutation, c.333_334ins(A) variant was selected, which leads to a frameshift mutation. I used PEs to install an LNS disease model and recover disease-causing mutations (Fig. 10). To generate an LNS disease model, a pegRNA encoding the desired A insertion was designed. The 12 pegRNAs with various RT(11-17nt)-PBS(10-16nt) lengths for c.333_334ins(A) mutation were designed (Fig. 11). The ngRNA was designed to cause a nick to occur in the non-edited strand 99nt upstream of the pegRNA induced nick location. Also, to correct an LNS causing mutation, I designed 15 pegRNAs containing different PBS(9-16nt) and RT(8-18nt) lengths to edit the desired A deletion (Fig. 11). The pegRNAs optimization was conducted to find the most efficient PE system for further studies. Several pegRNA encoding the desired A insertion plasmid and prime editor 2(PE2) were co-transfected in HEK293T cell. After that, targeted deep sequencing was used to examine the efficiency of prime editing. Deep sequencing revealed that the PBS length of 12 nucleotide(nt) and a RT template length of 15nt of pegRNA was best editing efficiency. (Fig. 12A). When tested in cultured mammalian cells, PE3 and PE3b editing efficiency would be higher than that of PE2.[18] Therefore, I tried to use PE3 or PE3b for genome editing by introducing a sgRNA. As a result, when the PE3b system was used, the highest efficiency was shown at 7.6% (Fig. 12B), which was selected and used in subsequent experiments. To select efficient pegRNAs to correct disease mutations, several pegRNA plasmid and PE2 were co-transfected in *HPRT1* mutant-HEK293T cell. The three pegRNAs with the highest efficiency were selected. (Fig. 13A). As in previous studies, the most efficient pegRNA was selected through comparison of PE2 and PE3b activity tests. The highest editing frequency of pegRNA was 46.7% with 11-

nt PBS and 10-nt RT using PE3b systems (Fig. 13B) and used in subsequent experiments. To establish deficient and rescued cell lines, HAP1 cells and *HPRT1* deficient HAP1 cells were transfected with the PE2, selected pegRNA and sgRNA. The transfected cell was then treated with 6-TG and HAT drug and confirmed the installed cells accurately edited. Sanger sequencing showed (A) insertion and (A) deletion from mutant and rescued cell lines, respectively (Fig. 14). In silico analysis revealed no detectable off-target mutations at 3 potential off-target sites (Fig. 15). The broken and recovered HPRT1 function may be proved by selecting 6-TG and HAT drug (Fig. 16) and confirming HPRT1 protein expression (Fig. 17). I found that disease modeling and correction of LNS disease related variations can be done successfully with the prime editors.

A

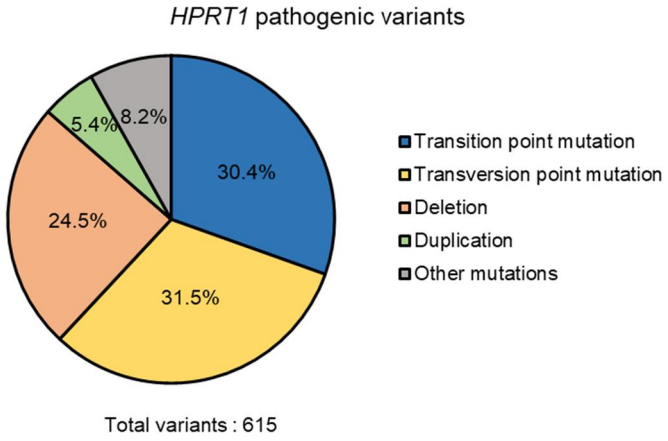

B

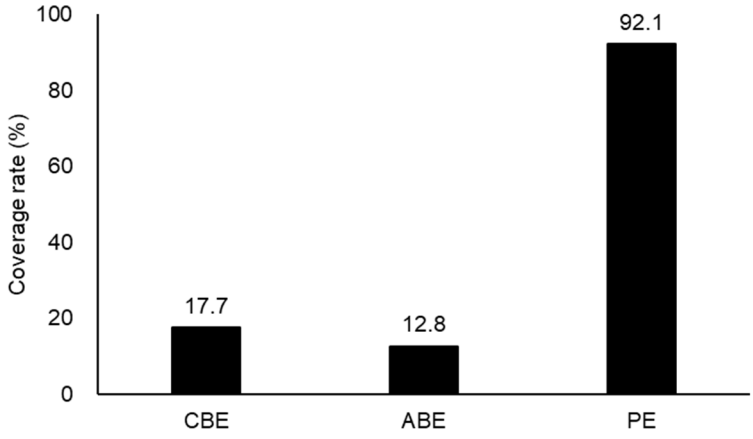

Figure 1. *HPRT1* mutation analysis in worldwide databases.

(A) The overall spectrum of type classification for all 615 *HPRT1* variants reported in the LNS database to date.

(B) Coverage frequency that can target *HPRT1* mutation using CBE, ABE, and PE construct theoretically.

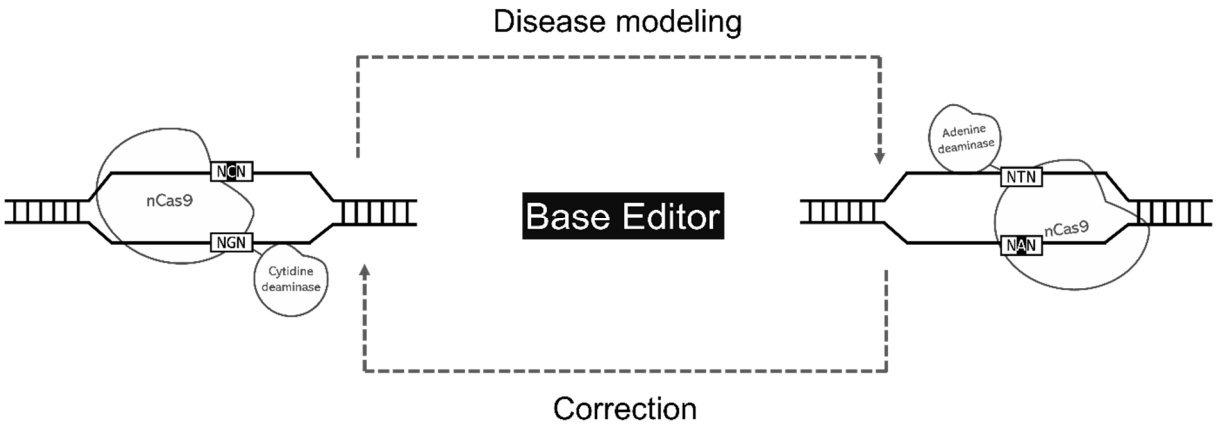

Figure 2. Overview of disease modeling and correction by base editor.

The overall scheme of generating point mutation using a base editor to perform genetic disorder modeling and correction.

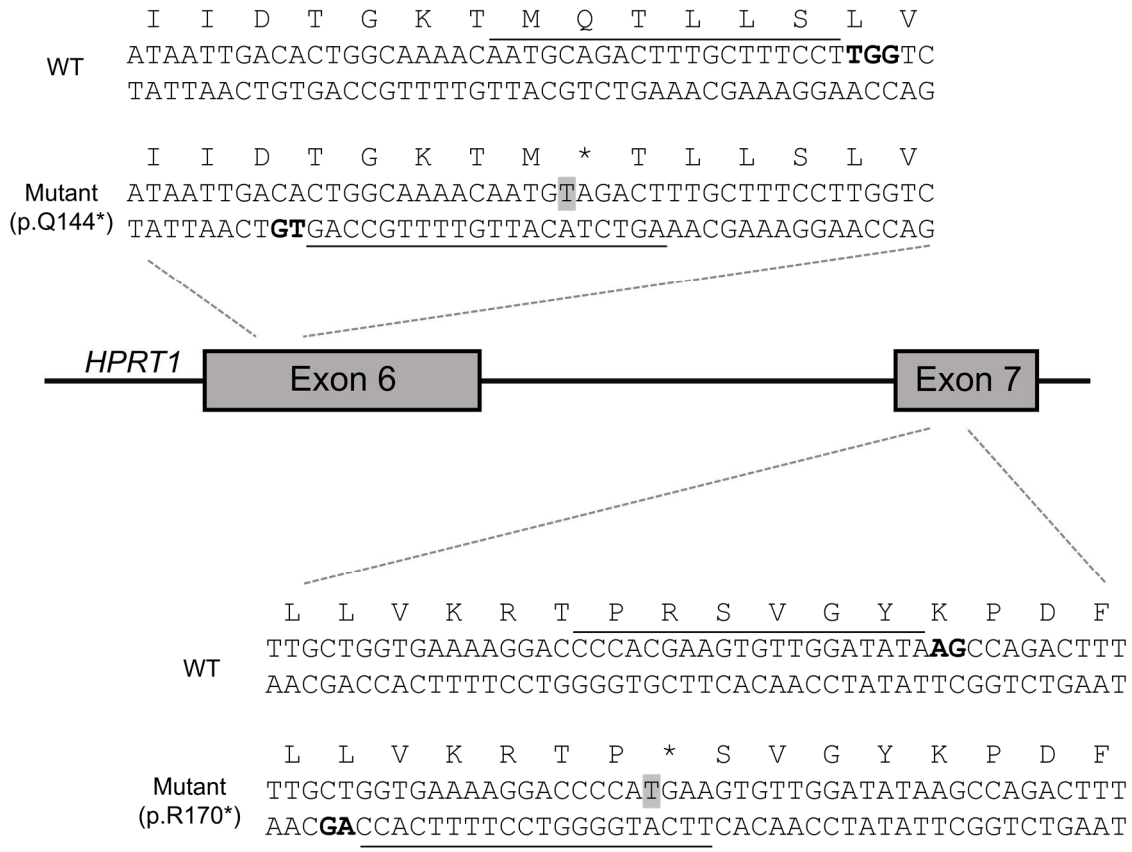

Figure 3. Wild type and mutant type gRNA design targeting *HRPT1* gene.

Scheme showing the target site sequence for two variants of c.430C>T and c.508C>T in *HPRT1* locus. Wild type and mutant type protospacer represent black underline and PAM sequences are bold letter. The LNS-related variant nucleotides are highlighted. The C to T substitutions lead to premature stop codon which is shown star.

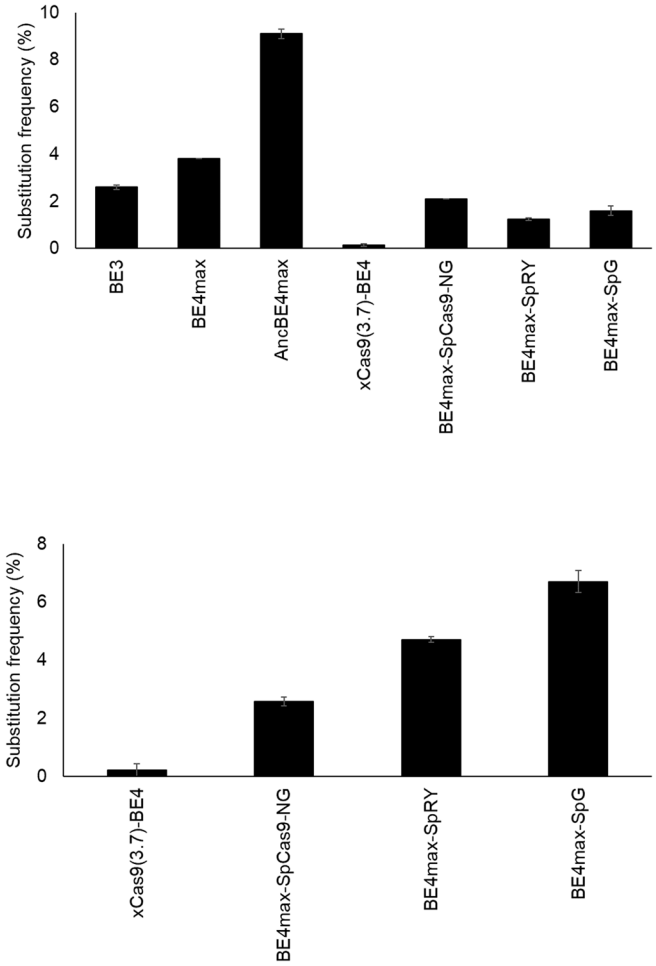

Figure 4. Optimization of base editors for *HPRT1* variants mutation editing.

Comparison of C to T editing efficiency using various base editors for two variants of *HPRT1* locus in HEK293T/17 cell.

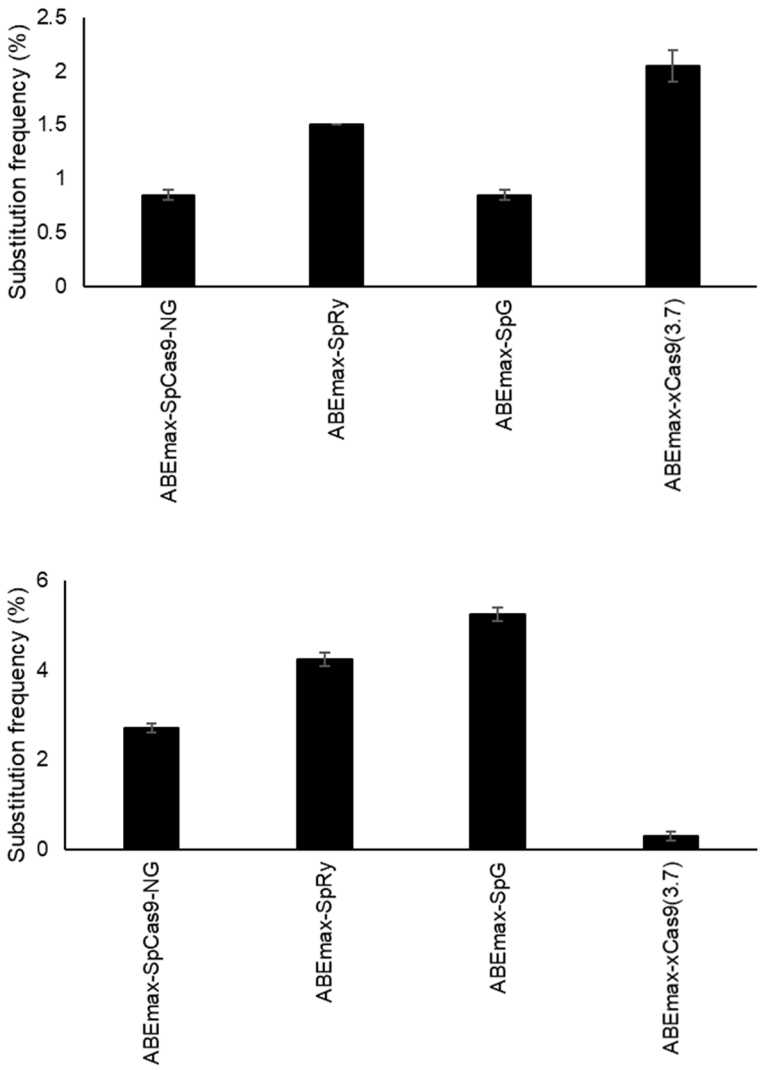

Figure 5. Optimization of base editors for *HPRT1* variants rescue editing.

Comparison of rescue editing efficiency using various base editors for two variants of *HPRT1* locus in *HPRT1* mutant-HEK293T/17 cell.

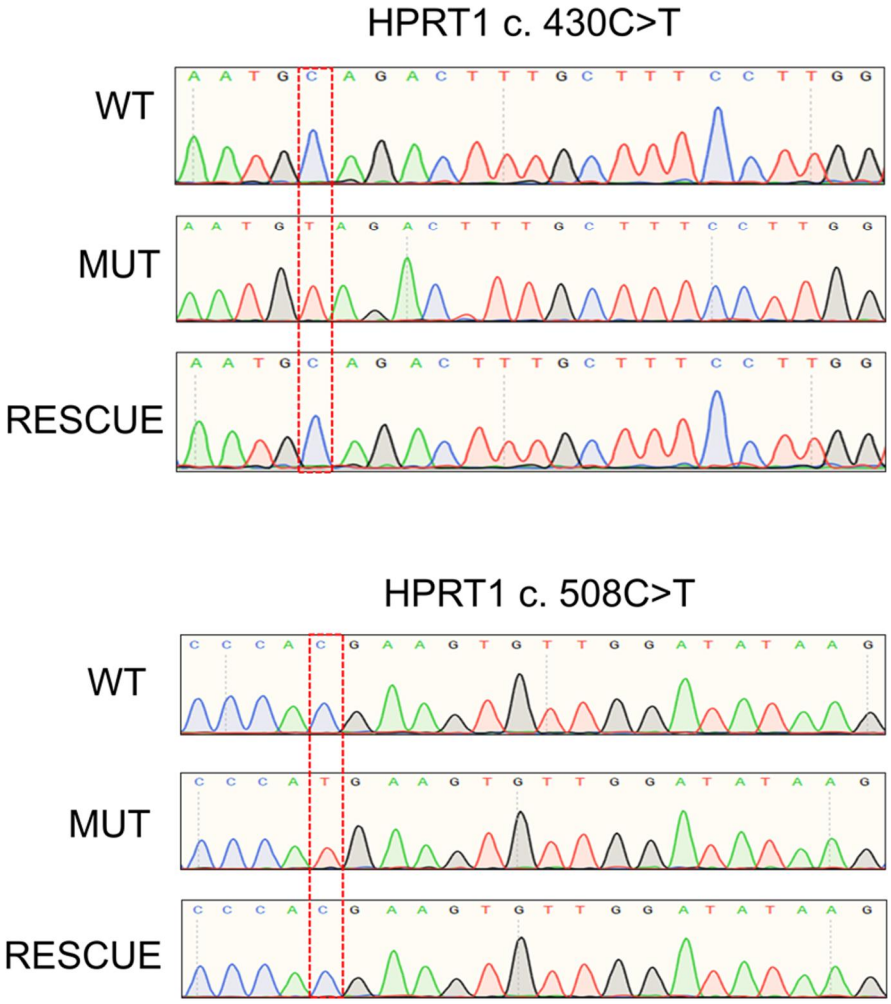

Figure 6. Sanger sequencing results in *HPRT1* variants.

Sanger sequencing results in gDNA extracted from defective cell lines and rescued cell lines for two variations of *HPRT1*. The change in C to T and T to C substitution induced by base editing is expressed in dashed red box.

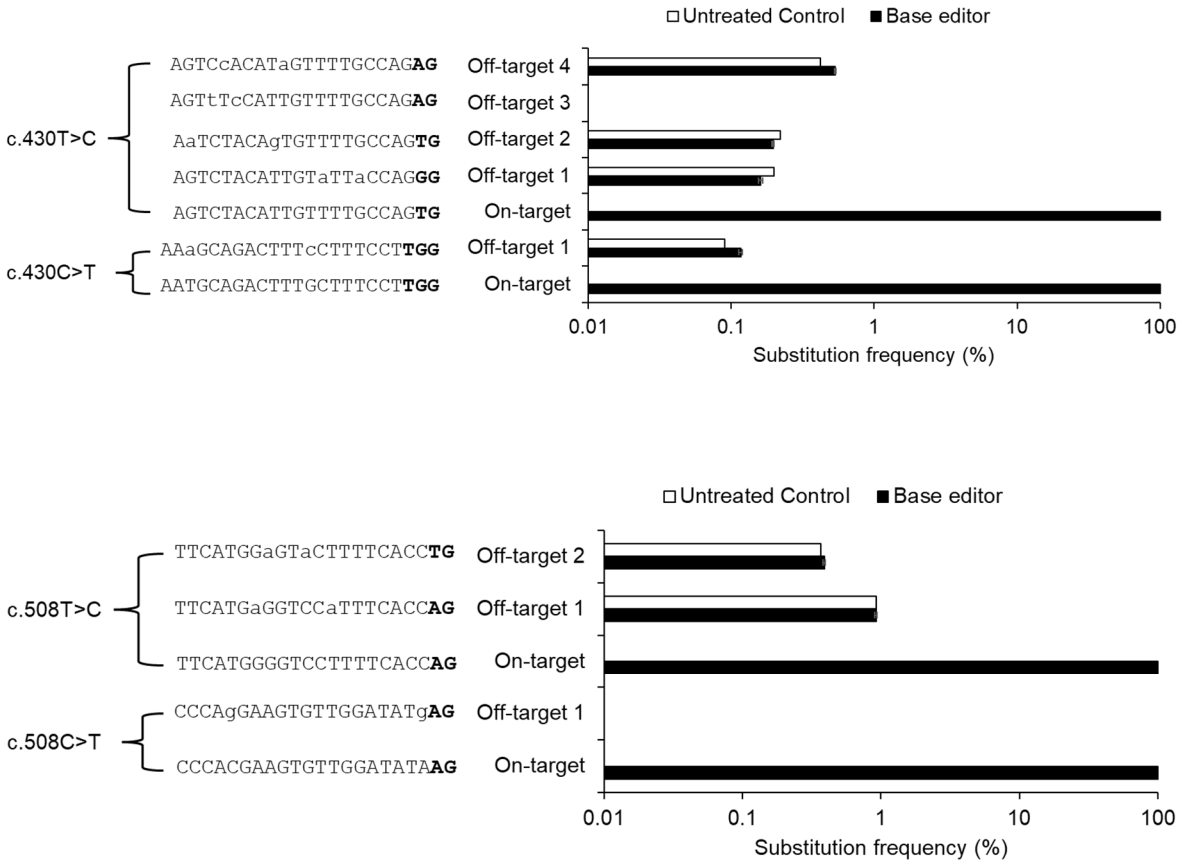

Figure 7. Targeted deep sequencing outcomes to analysis off-target effects from *HPRT1* mutant and rescued cell lines.

On-target and off-target efficiency of triplicate on average in mutant cell lines and rescued cell lines for *HPRT1* c.430C>T, c.508C>T mutations. The potential off-target site is predicted by the Cas-OFFinder online tool. The spacer sequence of mismatch≤2 is considered a potential off target site. The mismatch sequence of the target site is shown in lower case letters and the PAM sequence is in bold letters.

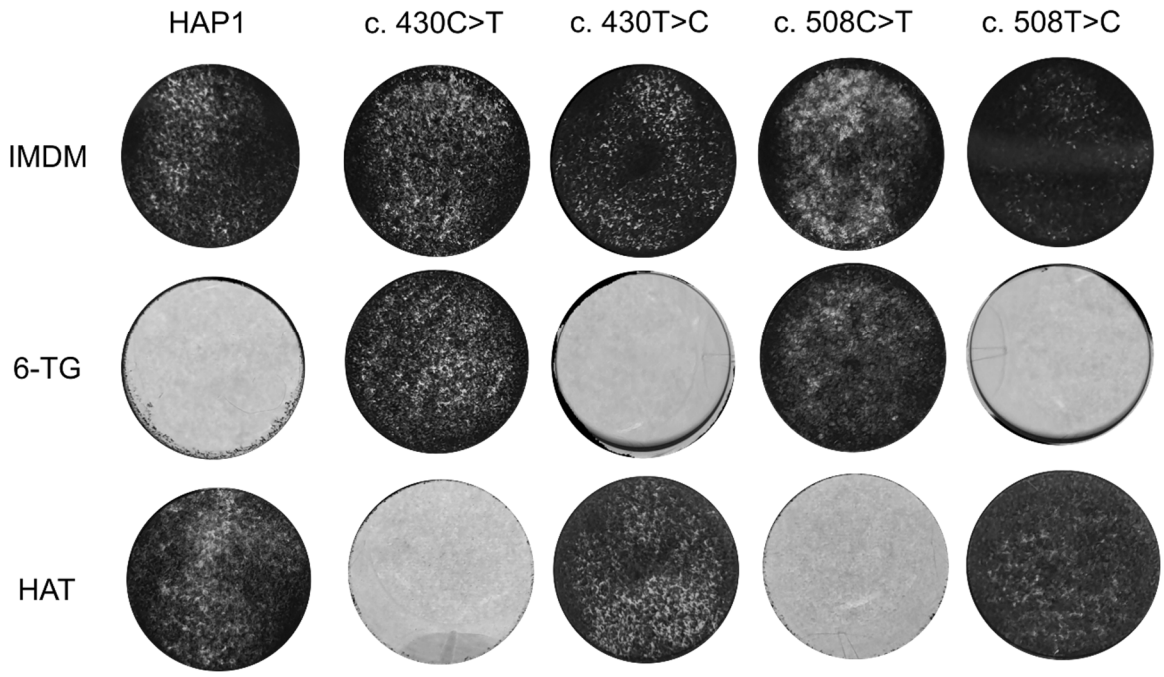

Figure 8. Crystal violet staining of drug-selected mutant and rescued cell lines.

Crystal violet staining of cells selected using 6-TG and HAT with mutant cell lines and rescued cell lines for two mutations of *HPRT1*. The cell was seeded to 24well (1.5×10^5) and fixed to 4% paraformaldehyde and then stained with crystal violet.

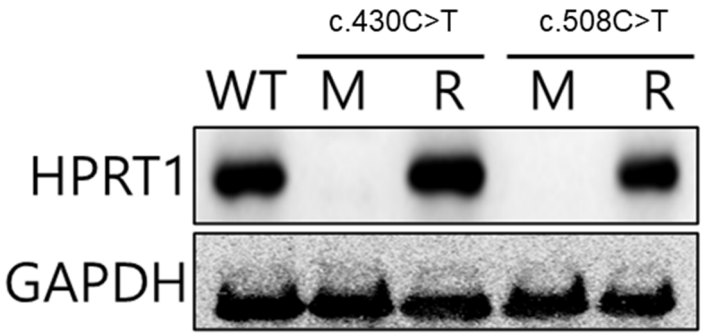

Figure 9. Identification of HPRT1 protein expression in established cell lines.

The protein expression of HPRT1 in mutant and rescued cell lines is confirmed by Western blot. GAPDH is used as the control of HPRT1. M and R represent mutant cell lines and rescued cell lines, respectively.

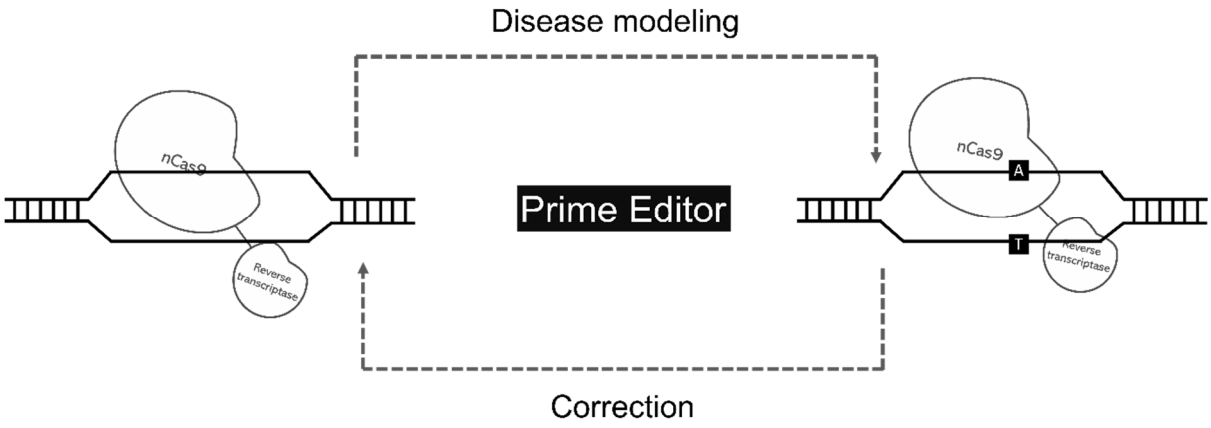

Figure 10. Overview of disease modeling and correction by prime editor.

The overall scheme of generating 1bp (A) insertion using a prime editor to perform genetic disorder modeling and correction.

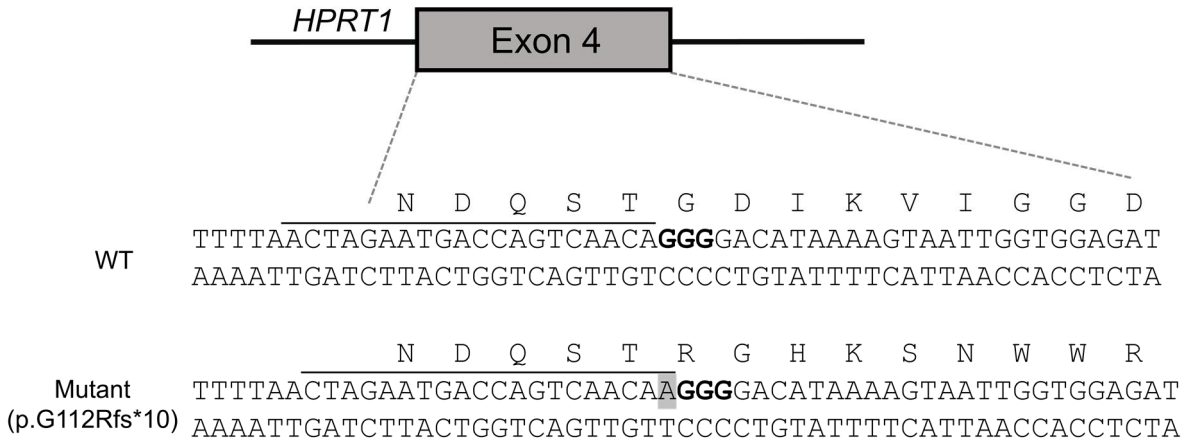

Figure 11. Wild type and mutant type pegRNA design targeting *HRPT1* gene.

The target and neighboring sequence in exon 4 of *HPRT1*. Wild type and mutant type protospacer represent black underline and PAM sequences are bold letter. The LNS-related A nucleotides are highlighted.

A

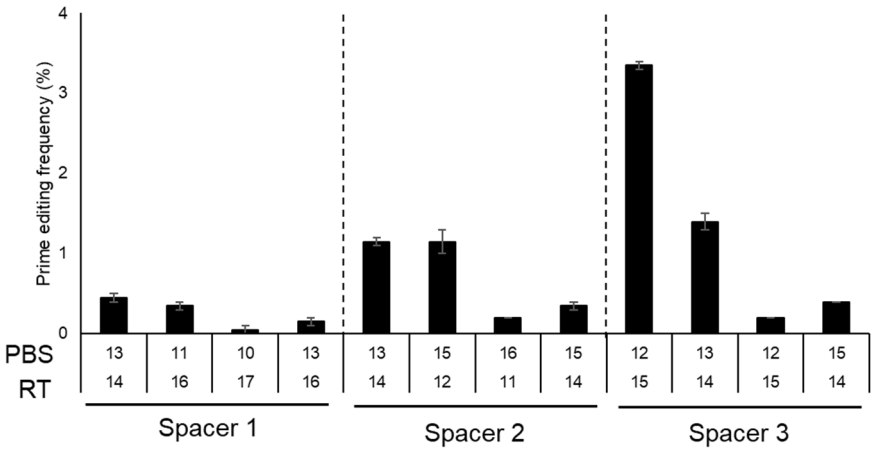

B

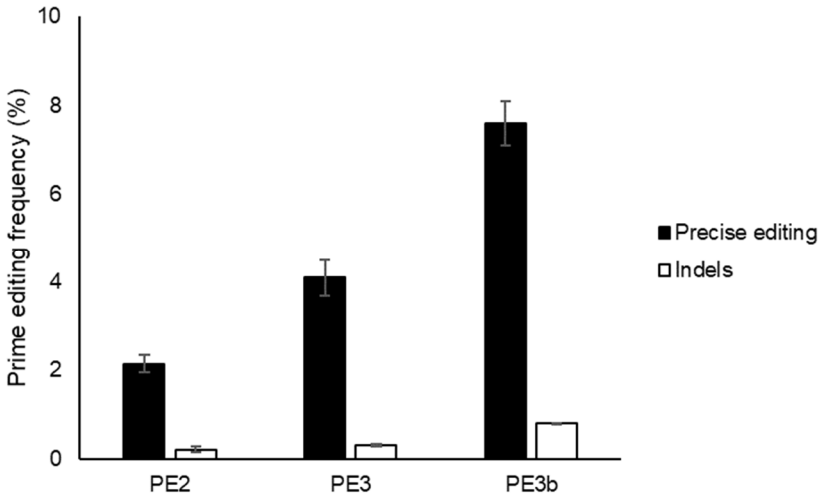

Figure 12. Optimization of pegRNAs for *HPRT1* variant mutation editing.

(A) PE2 efficiency comparison for *HPRT1* c.333_334ins(A) mutation editing to optimize pegRNAs with various PBS-RT lengths.

(B) Comparison of PE2, PE3, and PE3b editing efficiency by selecting pegRNA with the highest editing efficiency.

A

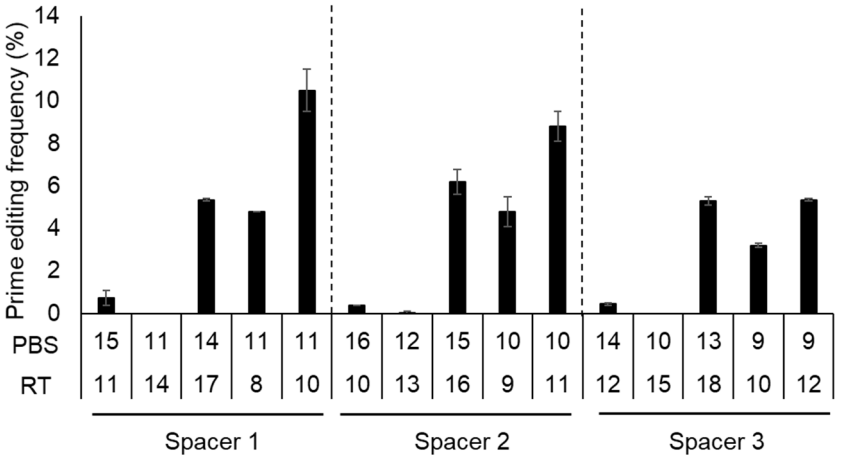

B

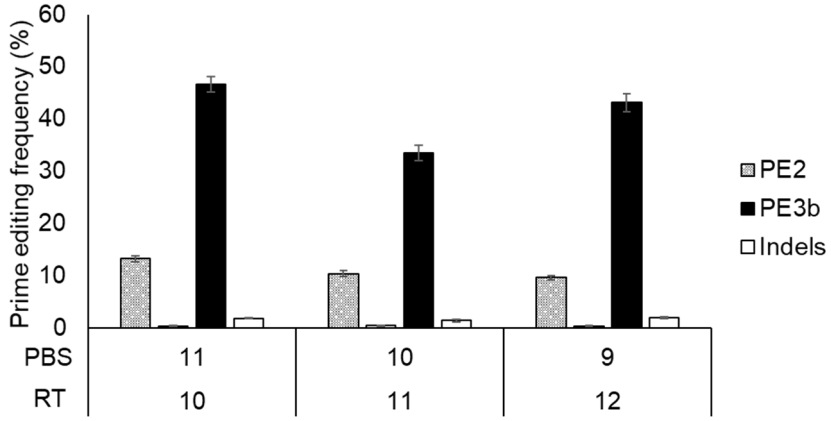

Figure 13. Optimization of pegRNAs for *HPRT1* mutation rescue editing.

(A) PE2 efficiency comparison for *HPRT1* mutation rescue editing to optimize pegRNAs with various PBS-RT lengths.

(B) Comparison of PE2 and PE3b editing efficiency by selecting pegRNA with the highest editing efficiency.

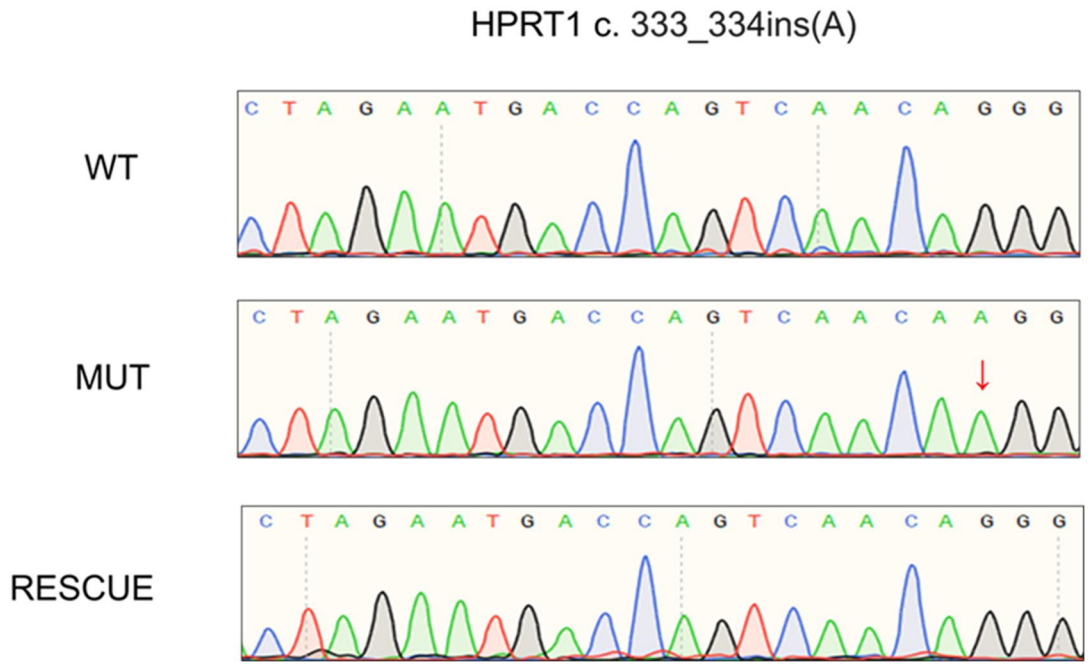

Figure 14. Sanger sequencing results in *HPRT1* variants.

Sanger sequencing results in gDNA extracted from mutant cell lines and rescued cell lines for (A) insertion mutation. The red arrow denotes (A) insertion induced by prime editing.

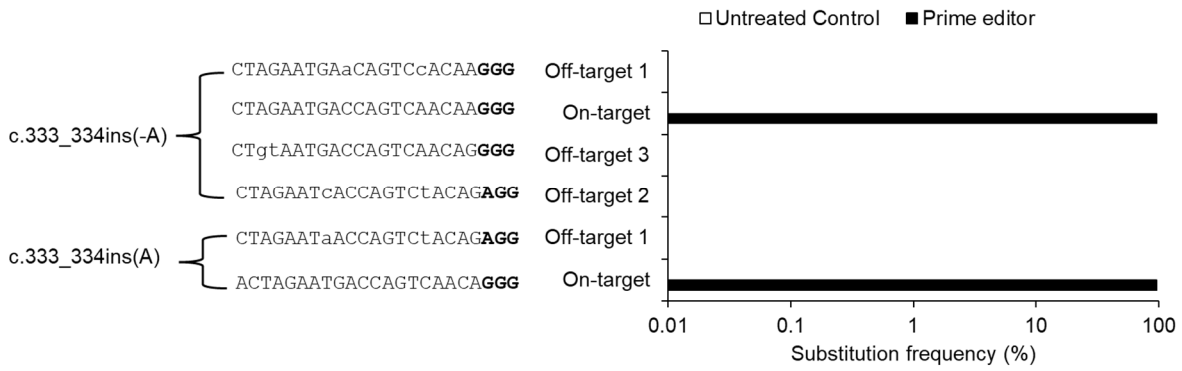

Figure 15. Targeted deep sequencing outcomes to analysis off-target effects from *HPRT1* mutant and rescued cell lines.

On-target and off-target efficiency of triplicate on average in mutant cell lines and rescued cell lines for *HPRT1* c.333_33ins(A) mutations. The potential off-target site is predicted by the Cas-OFFinder online tool. The space sequence of mismatch≤2 is considered a potential off target site. The mismatch sequence of the target site is shown in lower case letters and the PAM sequence is in bold letters.

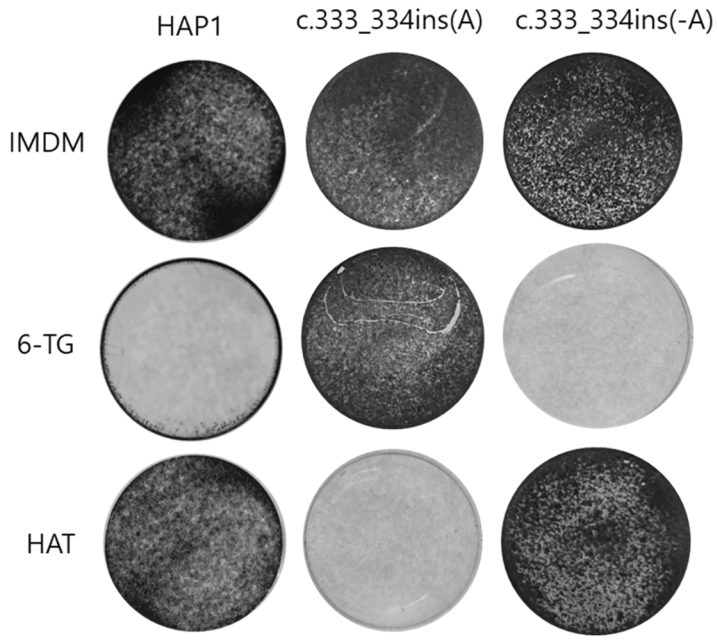

Figure 16. Crystal violet staining of drug-selected mutant and rescued cell lines.

Crystal violet staining of cells selected using 6-TG and HAT with mutant cell lines and recued cell lines for two mutations of *HPRT1*. The cell was seeded to 24well (1.5×10^5) and fixed to 4% paraformaldehyde and then stained with crystal violet.

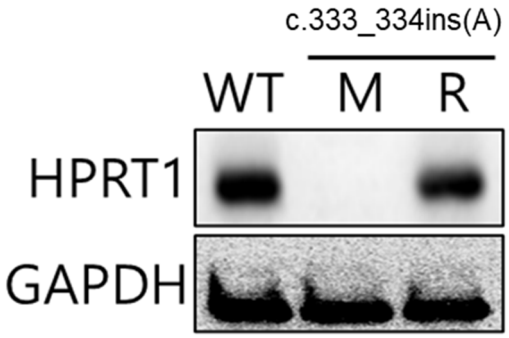

Figure 17. Identification of HPRT1 protein expression in established cell lines.

The protein expression of HPRT1 in mutant and rescued cell lines is confirmed by Western blot. GAPDH is used as the control of HPRT1. M and R represent mutant cell lines and rescued cell lines, respectively.

Table 1. Sequences list of each gRNA used in this study.

Target gene	Target sequence (5' to 3' w/ PAM)
HPRT1 c.430C>T	AATGCAGACTTTGCTTTCCTTGG
HPRT1 c.430T>C	AGTCTACATTGTTTTGCCAGTG
HPRT1 c.508C>T	CCCACGAAGTGTTGGATATAAG
HPRT1 c.508T>C	TTCATGGGGTCCTTTTCACCAG

Table 2. Sequences of pegRNA including PBS length and RT template length.

pegRNA	spacer sequence	3' extension	PBS length(nt)	RT template length(nt)
HRPT1 c.333_334ins(A)	AACTAGAATGACCAGTCAAC	TATGTCCCCTTGTTGACTGGTCATTCT	13	14
	AACTAGAATGACCAGTCAAC	TTTATGTCCCCTTGTTGACTGGTCATT	11	16
	AACTAGAATGACCAGTCAAC	TTTTATGTCCCCTTGTTGACTGGTCAT	10	17
	AACTAGAATGACCAGTCAAC	TTTATGTCCCCTTGTTGACTGGTCATTCT	13	16
	ACTAGAATGACCAGTCAACA	TATGTCCCCTTGTTGACTGGTCATTCT	14	13
	ACTAGAATGACCAGTCAACA	TTTATGTCCCCTTGTTGACTGGTCATT	12	15
	ACTAGAATGACCAGTCAACA	TTTTATGTCCCCTTGTTGACTGGTCAT	11	16
	ACTAGAATGACCAGTCAACA	TTTATGTCCCCTTGTTGACTGGTCATTCT	14	15
	CTAGAATGACCAGTCAACAG	TATGTCCCCTTGTTGACTGGTCATTCT	15	12
	CTAGAATGACCAGTCAACAG	TTTATGTCCCCTTGTTGACTGGTCATT	13	14
	CTAGAATGACCAGTCAACAG	TTTTATGTCCCCTTGTTGACTGGTCAT	12	15
	CTAGAATGACCAGTCAACAG	TTTATGTCCCCTTGTTGACTGGTCATTCT	15	14
HRPT1 c.333_334ins(-A)	CTAGAATGACCAGTCAACAA	TTTTATGTCCCCTGTTGACTGGTCA	15	11
	CTAGAATGACCAGTCAACAA	TACTTTTATGTCCCCTGTTGACTGGTCATTC	11	14
	CTAGAATGACCAGTCAACAA	TATGTCCCCTGTTGACTGGTCATTCT	14	17
	CTAGAATGACCAGTCAACAA	TGTCCCCTGTTGACTGGTC	11	8
	CTAGAATGACCAGTCAACAA	TATGTCCCCTGTTGACTGGTC	11	10
	TAGAATGACCAGTCAACAAG	TTTTATGTCCCCTGTTGACTGGTCA	16	10
	TAGAATGACCAGTCAACAAG	TACTTTTATGTCCCCTGTTGACTGGTCATTC	12	13
	TAGAATGACCAGTCAACAAG	TATGTCCCCTGTTGACTGGTCATTCT	15	16
	TAGAATGACCAGTCAACAAG	TGTCCCCTGTTGACTGGTC	10	9
	TAGAATGACCAGTCAACAAG	TATGTCCCCTGTTGACTGGTC	10	11
	ACTAGAATGACCAGTCAACA	TTTTATGTCCCCTGTTGACTGGTCA	14	12
	ACTAGAATGACCAGTCAACA	TACTTTTATGTCCCCTGTTGACTGGTCATTC	10	15
	ACTAGAATGACCAGTCAACA	TATGTCCCCTGTTGACTGGTCATTCT	13	18
	ACTAGAATGACCAGTCAACA	TGTCCCCTGTTGACTGGTC	9	10
	ACTAGAATGACCAGTCAACA	TATGTCCCCTGTTGACTGGTC	9	12

Table 3. List of nicking sgRNA for PE3 and PE3b.

nicking sgRNA	spacer sequence
HRPT1 c.333_334ins(A)_+99	CACACTGTTACTAATTGACT
HRPT1 c.333_334ins(A)_PE3b	TTTTATGTCCCCTTGTTGAC
HRPT1 c.333_334ins(-A)_PE3b	CTTTTATGTCCCCTGTTGAC

Table 4. List of off-target sites in *HPRT1* mutant and rescued cell types.

		Target sequences	Chr.	Position	MM
c.333_334ins(A)	On-target site	ACTAGAATGACCAGTCAACA **GGG**			
	Off-target 1	CTAGAATaACCAGTCtACAG **AGG**	chr5	17462867	2
	Off-target 2	CTAGAATcACCAGTCtACAG **AGG**	chr5	18120479	
	Off-target 3	CTgtAATGACCAGTCAACAG **GGG**	chr11	93998891	
c.333_334ins(-A)	On-target site	CTAGAATGACCAGTCAACAA **GGG**			
	Off-target 1	CTAGAATGAaCAGTCcACAA **GGG**	chr3	111068078	2
c.430C>T	On-target site	AATGCAGACTTTGCTTTCCT **TGG**			
	Off-target 1	AAaGCAGACTTTcCTTTCCT **TGG**	chr4	85585693	2
c.430T>C	On-target site	AGTCTACATTGTTTTGCCAG **TG**			
	Off-target 1	AGTCTACATTGTaTTaCCAG **GG**	chr9	24933903	2
	Off-target 2	AaTCTACAgTGTTTTGCCAG **TG**	chr6	80247927	
	Off-target 3	AGTtTcCATTGTTTTGCCAG **AG**	chr10	79115945	
	Off-target 4	AGTCcACATaGTTTTGCCAG **AG**	chr10	127863210	
c. 508C>T	On-target site	CCCACGAAGTGTTGGATATA **AG**			
	Off-target 1	CCCAgGAAGTGTTGGATATg **AG**	chr5	109184416	2
c. 508T>C	On-target site	TTCATGGGGTCCTTTTCACC **AG**			
	Off-target 1	TTCATGaGGTCCaTTTCACC **AG**	chr14	49402718	2
	Off-target 2	TTCATGGaGTaCTTTTCACC **TG**	chr4	67638721	

Table 5. Primer list for targeted deep sequencing.

Target gene	Primer name	Forward	Reverse
HPRT1 333_334ins(A)	1st	TCAGTAATGGCCGATTAGGAC	CCTAGACTGCTTCCAAGGGTTA
	2nd	ACACTCTTTCCCTACACGACGCTCTTCCGATCTTTGAAGTTTGTGTGTGTACATAAGGA	GTGACTGGAGTTCAGACGTGTGCTCTTCCGATCTCCCATTTAGTTATACTATGTAAATTATCTC
HPRT1 c.430C>T	1st	GGCTGGCATTCTTACTGCTT	CTGCCATGCTATTCAGGACA
	2nd	ACACTCTTTCCCTACACGACGCTCTTCCGATCTACATGGGGGTTTTGGTACTTT	GTGACTGGAGTTCAGACGTGTGCTCTTCCGATCTCCCCCTTCAAATGAGGAAA
HPRT1 c.508C>T	1st	GTCCTTCAGGTTCCAGGTGA	TCAAGGGCATATCCTACAACAA
	2nd	ACACTCTTTCCCTACACGACGCTCTTCCGATCTGTCTTCTCTTTTGTAATGCCCTGT	GTGACTGGAGTTCAGACGTGTGCTCTTCCGATCTACTGGCAAATGTGCCTCTCT
HPRT1 333_334ins(A) off-target 1	1st	CCTTCCGGTACTCCAATCAA	AAAACCCAAAAGGCCAGAGT
	2nd	ACACTCTTTCCCTACACGACGCTCTTCCGATCTGCAAGGTGGTCTTCCAACTC	GTGACTGGAGTTCAGACGTGTGCTCTTCCGATCTGGGGCACAGAACTAGATAGGG
HPRT1 333_334ins(A) off-target 2	1st	GATGGAGGATCAGATGACGAA	TTATCGAAGGCCTTTTCTGC
	2nd	ACACTCTTTCCCTACACGACGCTCTTCCGATCTCCCAATGCAAAGAAGCTAAGA	GTGACTGGAGTTCAGACGTGTGCTCTTCCGATCTTCCCATATTCCTTGCAGACTTT
HPRT1 333_334ins(A) off-target 3	1st	GGGCATATCCTGCAACAAGT	AGCCCCAGCATCATGATTAG
	2nd	ACACTCTTTCCCTACACGACGCTCTTCCGATCTGTTGGCATTGTTTTGCCAGT	GTGACTGGAGTTCAGACGTGTGCTCTTCCGATCTTGCCTGAGATGTGATGAAGG
HPRT1 c. 333_334ins(-A) off-target 1	1st	CTCCTTGCCTTCTTCCATGA	CAAACTGCAAAATCGCAGAA
	2nd	ACACTCTTTCCCTACACGACGCTCTTCCGATCTCAGGCTCGTCTTGAACTCCT	GTGACTGGAGTTCAGACGTGTGCTCTTCCGATCTGCTCTCCAGGACCACATCAT
HPRT1 c.430C>T off-target 1	1st	CTCTGGCACTCACCACTCAC	GGCACTTTTCCCTTCTGGAT
	2nd	ACACTCTTTCCCTACACGACGCTCTTCCGATCTTCATGGAATTGAGTAGATGGAAGA	GTGACTGGAGTTCAGACGTGTGCTCTTCCGATCTGGGGAACCAAAGGTAGGAAA
HPRT1 c.430T>C off-target 1	1st	TCCCAATGTATTCCTGACTTGA	GACTGATTCAAGGATGAGCAGA
	2nd	ACACTCTTTCCCTACACGACGCTCTTCCGATCTTTCCAATGACTGAAACTCTTCG	GTGACTGGAGTTCAGACGTGTGCTCTTCCGATCTTGTCCATATTGGCTTGTTTTTG
HPRT1 c.430T>C off-target 2	1st	TCTTGAGGTGACCCCTGTTC	TGGACACTGTGGTGCTGACT
	2nd	ACACTCTTTCCCTACACGACGCTCTTCCGATCTGTGGAAGTCTATGTTGTGATGAGG	GTGACTGGAGTTCAGACGTGTGCTCTTCCGATCTTTCAAAAACTCTGAGGCAAGC
HPRT1 c.430T>C off-target 3	1st	ACTCACCTGAGGTTGGATGG	CAGAGCAGGCTTCAGGGTAG
	2nd	ACACTCTTTCCCTACACGACGCTCTTCCGATCTGCCCACTCTGTCTGGCATTA	GTGACTGGAGTTCAGACGTGTGCTCTTCCGATCTGGTGCAGTAAGGGGCTACAG
HPRT1 c.430T>C off-target 4	1st	GAGGCCCAAAGAGGAAGAGT	TTCTGTGTCTGGTCCCCATT
	2nd	ACACTCTTTCCCTACACGACGCTCTTCCGATCTCACCCCACTCAAGAACCACT	GTGACTGGAGTTCAGACGTGTGCTCTTCCGATCTCAAGTCAGGGCACAACAAGA
HPRT1 c.508C>T off-target 1	1st	TACTCCCACCCTTCCCATCT	CCAGTGCCAAATACTGCTGA
	2nd	ACACTCTTTCCCTACACGACGCTCTTCCGATCTCTCTCTTCACCCACCTCAGC	GTGACTGGAGTTCAGACGTGTGCTCTTCCGATCTGCAGCTTACAGGAAATGGAAA
HPRT1 c.508T>C off-target 1	1st	GTCCCACAGGTCCTAAACCA	CAGCATCAAATGGAAAACCA
	2nd	ACACTCTTTCCCTACACGACGCTCTTCCGATCTCCACCCCATTCGTGATTAAA	GTGACTGGAGTTCAGACGTGTGCTCTTCCGATCTGGAAATGCTGGGGGAATAAT
HPRT1 c.508T>C off-target 2	1st	GTGGGACTCACCCCAAAGTA	TGTCCAACCACTGAGACCAT
	2nd	ACACTCTTTCCCTACACGACGCTCTTCCGATCTAAAAACAAAAGACAGCCAAAAA	GTGACTGGAGTTCAGACGTGTGCTCTTCCGATCTCCTCAAACACAAACCCTTTGA

Discussion

LNS is rare disease caused by *HPRT1* mutation and LNS patients have no fundamental treatment and use drugs to relieve pain such as allopurinol [4]. So, I targeted the *HPRT1* gene that generates LNS using CRISPR-mediated genome editing technology for correcting mutation.

Targeting most *HPRT1* pathogenic mutations is possible using BEs and PEs construct with no restrictions on NGG PAM to overcome the limitations of PAM sequence. Thus, it is not a problem to target most LNS causing *HPRT1* mutations. BE and PE were applied for C to T and (A) insertion mutations with three patient-derived mutations. For each variation, an optimization test was performed to select an efficient BEs and pegRNA before establishing a mutant cell line and a recused cell line. Since the prime editing efficiency varies according to the target gene and cell types [18], the pegRNAs optimization are essential. To generate mutant and recused cell lines, selected BEs and pegRNA were transfected in near haploid HAP1 cell with gRNA and prime editing device, respectively. After all, the HPRT1 function was verified by treating 6-TG and HAT drug in the installed cell line and identified that the broken HPRT1 function was successfully repaired using BEs and PEs.

Correctively, I have demonstrated the feasibility of LNS disease modeling and repair of *HPRT1* genetic disorders in cells. Additionally, further experiments also confirmed that CRISPR-based prime editors could successfully correct the *HPRT1* mutation in LNS-patient-derived fibroblasts. Recently, PE has been developed that can increase efficiency and introduce mutations of various sizes [30-31], and it will be possible to repair LNS patient cells more efficiently without inducing off target effect. After that,

it is expected to be applicable to clinical trials through in vivo animal model studies. Therefore, CRISPR technology is expected to be used as a therapeutic agent for LNS genetic diseases in the future.

Reference

1. Lesch, M., & Nyhan, W. L. (1964). A familial disorder of uric acid metabolism and central nervous system function. The American journal of medicine, 36, 561–570.

2. Torres, R. J., & Puig, J. G. (2007). Hypoxanthine-guanine phosophoribosyltransferase (HPRT) deficiency: Lesch-Nyhan syndrome. Orphanet journal of rare diseases, 2, 48.

3. Kelley, W. N., Greene, M. L., Rosenbloom, F. M., Henderson, J. F., & Seegmiller, J. E. (1969). Hypoxanthine-guanine phosphoribosyltransferase deficiency in gout. Annals of internal medicine, 70(1), 155–206.

4. Rinat, C., Zoref-Shani, E., Ben-Neriah, Z., Bromberg, Y., Becker-Cohen, R., Feinstein, S., Sperling, O., & Frishberg, Y. (2006). Molecular, biochemical, and genetic characterization of a female patient with Lesch-Nyhan disease. Molecular genetics and metabolism, 87(3), 249–252.

5. Fox, I. H., & Kelley, W. N. (1971). Phosphoribosylpyrophosphate in man: biochemical and clinical significance. Annals of internal medicine, 74(3), 424–433.

6. Bell, S., Kolobova, I., Crapper, L., & Ernst, C. (2016). Lesch-Nyhan Syndrome: Models, Theories, and Therapies. Molecular syndromology, 7(6), 302–311.

7. Nyhan W. L. (2005). Lesch-Nyhan Disease. Journal of the history of the

neurosciences, 14(1), 1-10.

8. Kantor, A., McClements, M. E., & MacLaren, R. E. (2020). CRISPR-Cas9 DNA Base-Editing and Prime-Editing. International journal of molecular sciences, 21(17), 6240.

9. Cho, S. W., Kim, S., Kim, J. M., & Kim, J. S. (2013). Targeted genome engineering in human cells with the Cas9 RNA-guided endonuclease. Nature biotechnology, 31(3), 230–232.

10. S Jinek, M., East, A., Cheng, A., Lin, S., Ma, E., & Doudna, J. (2013). RNA-programmed genome editing in human cells. eLife, 2, e00471.

11. Mao, Z., Bozzella, M., Seluanov, A., & Gorbunova, V. (2008). Comparison of nonhomologous end joining and homologous recombination in human cells. DNA repair, 7(10), 1765-1771.

12. Song, F., & Stieger, K. (2017). Optimizing the DNA Donor Template for Homology-Directed Repair of Double-Strand Breaks. Molecular therapy. Nucleic acids, 7, 53-60.

13. Anzalone, A. V., Koblan, L. W., & Liu, D. R. (2020). Genome editing with CRISPR-Cas nucleases, base editors, transposases and prime editors. Nature biotechnology, 38(7), 824-844.

14. Komor, A. C., Kim, Y. B., Packer, M. S., Zuris, J. A., & Liu, D. R. (2016). Programmable editing of a target base in genomic DNA without double-stranded DNA cleavage. Nature, 533(7603), 420-424.

15. Gaudelli, N. M., Komor, A. C., Rees, H. A., Packer, M. S., Badran, A. H., Bryson, D. I., & Liu, D. R. (2017). Programmable base editing of A•T to G•C in genomic DNA without DNA cleavage. Nature, 551(7681), 464-471.

16. Kim, K., Ryu, S. M., Kim, S. T., Baek, G., Kim, D., Lim, K., Chung, E., Kim, S., & Kim, J. S. (2017). Highly efficient RNA-guided base editing in mouse embryos. Nature biotechnology, 35(5), 435–437.

17. Ryu, S. M., Koo, T., Kim, K., Lim, K., Baek, G., Kim, S. T., Kim, H. S., Kim, D. E., Lee, H., Chung, E., & Kim, J. S. (2018). Adenine base editing in mouse embryos and an adult mouse model of Duchenne muscular dystrophy. Nature biotechnology, 36(6), 536–539.

18. Anzalone, A. V., Randolph, P. B., Davis, J. R., Sousa, A. A., Koblan, L. W., Levy, J. M., Chen, P. J., Wilson, C., Newby, G. A., Raguram, A., & Liu, D. R. (2019). Search-and-replace genome editing without double-strand breaks or donor DNA. Nature, 576(7785), 149-157.

19. Lin, Q., Zong, Y., Xue, C., Wang, S., Jin, S., Zhu, Z., Wang, Y., Anzalone, A. V.,

Raguram, A., Doman, J. L., Liu, D. R., & Gao, C. (2020). Prime genome editing in rice and wheat. Nature biotechnology, 38(5), 582–585.

20. Liu, Y., Li, X., He, S., Huang, S., Li, C., Chen, Y., Liu, Z., Huang, X., & Wang, X. (2020). Efficient generation of mouse models with the prime editing system. Cell discovery, 6(1), 27.

21. Liu, P., Liang, S. Q., Zheng, C., Mintzer, E., Zhao, Y. G., Ponnienselvan, K., Mir, A., Sontheimer, E. J., Gao, G., Flotte, T. R., Wolfe, S. A., & Xue, W. (2021). Improved prime editors enable pathogenic allele correction and cancer modelling in adult mice. Nature communications, 12(1), 2121.

22. Schene, I. F., Joore, I. P., Oka, R., Mokry, M., van Vugt, A., van Boxtel, R., van der Doef, H., van der Laan, L., Verstegen, M., van Hasselt, P. M., Nieuwenhuis, E., & Fuchs, S. A. (2020). Prime editing for functional repair in patient-derived disease models. Nature communications, 11(1), 5352.

23. Lin, J., Liu, X., Lu, Z., Huang, S., Wu, S., Yu, W., Liu, Y., Zheng, X., Huang, X., Sun, Q., Qiao, Y., & Liu, Z. (2021). Modeling a cataract disorder in mice with prime editing. Molecular therapy. Nucleic acids, 25, 494–501.

24. Official website of the Lesch-Nyhan disease Study Group. [http://www.lesch-nyhan.org]

25. Liao, S., Tammaro, M., & Yan, H. (2015). Enriching CRISPR-Cas9 targeted cells by co-targeting the HPRT gene. Nucleic acids research, 43(20), e134.

26. Gallagher, R. E., Ferrari, A. C., Zulich, A. W., Yen, R. W., & Testa, J. R. (1984). Cytotoxic and cytodifferentiative components of 6-thioguanine resistance in HL-60 cells containing acquired double minute chromosomes. Cancer research, 44(6), 2642-2653.

27. Pan, B. F., & Nelson, J. A. (1990). Characterization of the DNA damage in 6-thioguanine-treated cells. Biochemical pharmacology, 40(5), 1063-1069.

28. Swann, P. F., Waters, T. R., Moulton, D. C., Xu, Y. Z., Zheng, Q., Edwards, M., & Mace, R. (1996). Role of postreplicative DNA mismatch repair in the cytotoxic action of thioguanine. Science (New York, N.Y.), 273(5278), 1109-1111.

29. Freshney, R. I., Culture of Animal Cells: A Manual of Basic Technique, 3rd ed. (John Wiley & Sons, Inc.,1994) pp. 389-391.

30. Nelson, J. W., Randolph, P. B., Shen, S. P., Everette, K. A., Chen, P. J., Anzalone, A. V., An, M., Newby, G. A., Chen, J. C., Hsu, A., & Liu, D. R. (2021). Engineered pegRNAs improve prime editing efficiency. Nature biotechnology, 10.1038/s41587-021-01039-7.

31. Anzalone, A. V., Gao, X. D., Podracky, C. J., Nelson, A. T., Koblan, L. W., Raguram, A., Levy, J. M., Mercer, J., & Liu, D. R. (2021). Programmable deletion,

replacement, integration and inversion of large DNA sequences with twin prime editing. Nature biotechnology, 10.1038/s41587-021-01133-w.

국문요약

유전되는 인간의 유전적 장애는 대부분 관련 유전자 또는 그 조절 요소에서 뉴클레오타이드 변형에 의해 발생한다. 유전체에는 점 돌연변이, 삽입, 결실과 같은 다양한 형태의 뉴클레오타이드 변화가 있다. 살아있는 세포와 유기체에 이러한 뉴클레오티드 변화를 도입하고 수정하는 것은 인간의 유전 질환을 관리하는 데 큰 도전이다. 기존 크리스퍼 기반 핵산분해효소가 개발돼 다양한 유전질환과 연관된 유전자 치료에 광범위하게 적용됐지만 표적 돌연변이를 교정하기 위한 핵산분해효소 기반 유전자 편집은 교정빈도가 낮고 DNA 이중 가닥 절단 발생, 외부 DNA 템플릿 요구 등 여러 한계가 있다. 이러한 한계를 극복하기 위해, 최근 연구는 크리스퍼 매개 염기 교정 가위와 프라임 교정 가위가 유전체에서 원하는 돌연변이를 편집할 수 있다는 것을 보여준다.

희귀 유전질환으로 잘 알려진 레쉬-니한 증후군은 하이포잔틴-구아닌 포스포리보실전이효소 1 유전자 돌연변이에 의해 발생한다. HPRT1 결핍은 고혈증과 운동 기능 장애, 인지 장애, 행동 장애와 같은 다양한 신경학적 증상을 유발한다. 지난 50년 동안 HPRT1의 인과적 역할이 확인되었지만, LNS 환자에 대한 근본적인 치료법은 없다. 크리스퍼 기반 유전자 치료의 실현 가능성에 대한 개념 증명 증거를 제공하기 위해 크리스퍼 매개 염기 및 프라임 교정 가위를 적용하여 LNS 관련 HPRT1 유전자 돌연변이를 교정했다. 최적화된 염기 및 프라임 교정 가위로 c.333_334ins(A), c.430C>T, c.508C>T LNS 환자 유래 돌연변이를 도입한 세포 주 여러 개를 생성했다. 그런 다음 46.7% 효율로 세포 내 돌연변이를 수정하고 수정된 세포주를 생성했다. 나아가 이러한 확립된 세포 주 들에서 HPRT1의 기능을 분석해보니 돌연변이 세포에서 HPRT1의 기능이 완전히 망가졌고 교정된 세포에서 회복된 것을 확인했다. 이러한 결과에서 필자는 먼저 크리스퍼 매개 염기 및 프라임 교정 가위를 사용하여 LNS 모델

세포를 생성하고 HPRT1 유전자 교정을 통해 질병을 치료할 수 있도록 제안한다. 이러한 유전체 편집 도구는 LNS 환자의 다양한 유형의 유전자 돌연변이를 치료하는데 널리 사용될 수 있을 것이다.

Key word: 레쉬-니한 증후군, HPRT1, CRISPR-Cas9, 염기 교정 가위, 프라임 교정 가위, 유전자 편집, 유전자 치료